applied sciences

MDPI

Article

Ambient Backscatter- and Simultaneous Wireless Information and Power Transfer-Enabled Switch for Indoor Internet of Things Systems

Vishalya P. Sooriarachchi [1,2], Tharindu D. Ponnimbaduge Perera [3] and Dushantha Nalin K. Jayakody [1,2,4,*]

[1] COPELABS, Lusofona University, 1749-024 Lisbon, Portugal; a22211643@alunos.ulht.pt
[2] Center of Technology and Systems (UNINOVA-CTS) and LASI, 2829-516 Caparica, Portugal
[3] Faculty of Engineering & IT, The University of Melbourne, Melbourne, VIC 3053, Australia; tharindu.ponnimbadugeperera@unimelb.edu.au
[4] CIET/DEEE, Faculty of Engineering, Sri Lanka Institute of Information Technology, Malabe 10115, Sri Lanka
* Correspondence: dushantha.jayakody@ulusofona.pt

Abstract: Indoor Internet of Things (IoT) is considered as a crucial component of Industry 4.0, enabling devices and machine to communicate and share sensed data leading to increased efficiency, productivity, and automation. Increased energy efficiency is a significant focus within Industry 4.0, as it offers numerous benefits. To support this focus, we developed a hybrid switching mechanism to switch between energy harvesting techniques, ambient backscattering and Simultaneous Wireless Information and Power Transfer (SWIPT), which can be utilized within cooperative communications. To implement the proposed switching mechanism, we consider an indoor warehouse environment, where the moving sensor node transmits sensed data to the fixed relay located on the roof, which is then transmitted to an IoT gateway. The relay is equipped with the proposed switch to energize its communication capabilities while maintaining the expected quality of service at the IoT gateway. Simulation results illustrate the improved energy efficiency within the indoor communication setup while maintaining QoS at varying signal-to-noise (SNR) conditions.

Keywords: simultaneous wireless information and power transfer (SWIPT); ambient backscatter communication systems (ABCSs); wireless sensor networks; Internet of Things (IoT)

check for updates

Academic Editors: Alessandro Lo Schiavo and Pedro Couto

Received: 14 October 2024
Revised: 14 December 2024
Accepted: 24 December 2024
Published: 6 January 2025

Citation: Sooriarachchi , V.P.; Perera, T.D.P.; Jayakody, D.N.K. Ambient Backscatter- and Simultaneous Wireless Information and Power Transfer-Enabled Switch for Indoor Internet of Things Systems. *Appl. Sci.* **2025**, *15*, 478. https://doi.org/10.3390/app15010478

Copyright: © 2025 by the authors. Licensee MDPI, Basel, Switzerland. This article is an open access article distributed under the terms and conditions of the Creative Commons Attribution (CC BY) license (https://creativecommons.org/licenses/by/4.0/).

1. Introduction

The Internet of Things (IoT) has emerged as a cornerstone of the Industry 4.0 revolution, transforming industrial operations through real-time monitoring, control, and optimization [1]. In the context of Industry 4.0, IoT enables the creation of smart factories where interconnected devices and systems communicate seamlessly, allowing for real-time monitoring and control of manufacturing processes. These IoT-enabled environments support the implementation of cyber–physical systems, where industrial machinery and IoT technologies converge to create highly adaptive and efficient production lines. By leveraging IoT sensors and actuators throughout the industrial ecosystem, industrial environments achieve unprecedented levels of automation, optimize resource allocation, and implement predictive maintenance strategies, ultimately leading to increased productivity and reduced operational costs [2–4].

As industrial IoT networks scale up, the number of connected devices and their associated tasks increases. However, the energy available to these devices is limited due to their constrained battery capacities and the often remote or hard-to-reach deployment locations, making frequent battery replacement impractical [5]. This limitation, combined

with the drive towards zero-energy and self-powered IoT devices, underscores the need for innovative energy management and harvesting techniques [6,7]. Since data processing and transmission dominate energy consumption, minimizing overheads and extending battery life through efficient load balancing is essential for the longevity of industrial networks. Therefore, energy efficiency remains a dominant factor when establishing IoT networks within Industry 4.0 [4,8,9].

Among the promising solutions, ambient backscatter communication systems (ABCSs) and simultaneous wireless information and power transfer (SWIPT) have gained significant attention. The ABCS allows ultra-low-power communication by reflecting existing RF signals, eliminating the need for active RF components [10]. This technique is highly energy-efficient, though it faces limitations in communication range and data rate, with performance depending on the availability of ambient RF signals. The ABCS operates by altering the impedance of the antenna in a backscatter device, modulating the phase and amplitude of the reflected signal, which can then be decoded by a receiver tuned to the ambient signal. While ABCS is ideal for energy-constrained IoT devices due to its minimal power consumption, challenges related to limited range, data rate, and dependency on RF signal strength remain [11].

Conversely, SWIPT enables simultaneous data and power transmission, optimizing spectrum usage and facilitating zero-energy device development in IoT networks [12]. SWIPT, leveraging electromagnetic waves for dual purposes, allows simultaneous information and power transfer, beneficial in areas where direct power sources are impractical. The two main SWIPT protocols—time switching (TS-SWIPT) and power splitting (PS-SWIPT)—alternate between energy harvesting (EH) and information decoding (ID) periods, or split the received signal power for ID and EH in an optimized ratio [13].

In addition to ABCS and SWIPT, other energy harvesting mechanisms such as solar-, thermal-, and vibration-based methods have been explored to address the energy needs of IoT devices in industrial applications. Solar energy harvesting is well suited for environments with ample sunlight, converting solar radiation into usable electrical energy for IoT nodes [14]. Thermal energy harvesting, which captures waste heat generated in industrial settings, presents a valuable option for energy recovery in temperature-variant environments [15]. Additionally, vibration energy harvesting leverages ambient mechanical vibrations from machinery and equipment, converting them into power suitable for low-energy IoT devices [16]. Each of these mechanisms has unique advantages and challenges, depending on environmental conditions and application requirements.

While these alternative mechanisms hold potential, they do not consistently meet the varying energy demands of IoT devices across dynamic industrial environments. These energy harvesting methods may offer a more resilient and adaptive energy solution, but within the context of an industrial environment, the availability of solar or thermal energy is highly limited, while the IoT devices cannot operate under vibration energy without disrupting the transmission process. Thus, the development of a suitable EH mechanism within an IoT network requires a clear understanding of the overall potential of the selected method.

Recent research has explored the potential of combining ABCS and SWIPT to leverage their respective strengths. Several studies have proposed integrating ABCS and SWIPT in relay networks. While these approaches show promise in enhancing energy efficiency, they often rely on fixed configurations that may not adapt well to dynamic industrial environments. Furthermore, the complexity of implementing both technologies simultaneously may lead to increased hardware costs and potential reliability issues. These studies have also focused on optimizing various aspects of combined ABCS-SWIPT systems, such as power allocation, time scheduling, and antenna configurations [17–19]. While these studies

provide valuable insights into system performance optimization, they often make simplifying assumptions about channel conditions or network topology that may not hold in real-world industrial settings. Also, the combination of other transmission techniques, such as visible light communication with energy harvesting-enabled SWIPT, creates complexities in the hardware units, making them less feasible and more cost-inefficient [20].

Another strand of research has explored innovative modulation schemes and communication protocols for hybrid systems [21,22]. These approaches aim to improve spectral efficiency and energy harvesting capabilities. Yet, many of these proposed schemes require significant changes to existing hardware and protocols, potentially limiting their practical applicability in the near term.

Despite these advances, achieving a balance between energy efficiency and data transmission rate remains a challenge, especially in dynamic and complex industrial environments. There is a lack of in-depth analysis on how to optimize this balance and on how to select the optimal approach for different application scenarios. This challenge is further compounded by the need to ensure that IoT devices can dynamically adapt to changing energy availability and network demands without compromising performance.

Another aspect that has been studied is the use of systems with dynamic SWIPT ratio allocation. Although SWIPT offers flexibility in allocating signal power between EH and information decoding ID, its application in very-low-power environments presents specific limitations. In such settings, the power received may be insufficient to sustain both EH and ID simultaneously, even when dynamically adjusting the power split ratio. This limitation is particularly challenging in industrial environments where IoT devices operate with minimal power availability and may be reliant on inconsistent or weak RF sources. Additionally, continuous dynamic adjustments in the power splitting ratio to optimize energy and data needs can introduce higher processing overhead and complexity, which may be impractical for devices with limited computational resources. These constraints suggest that in ultra-low-power conditions, alternative or supplementary energy management techniques might be necessary to support consistent IoT device functionality [23–25].

To address these gaps, we propose a novel hybrid switching mechanism that dynamically selects between ABCS and SWIPT based on real-time channel conditions and energy requirements, optimizing for both energy efficiency and data transmission rate across various industrial scenarios. Unlike fixed configurations, our system makes adaptive choices between ABCS and SWIPT modes based on instantaneous environmental factors, allowing for flexible and optimal performance in diverse contexts. This approach not only enhances adaptability but also provides a practical framework for making energy–rate trade-offs in real time, ensuring that IoT devices maintain functionality even under fluctuating network demands. Additionally, we maintain a strong focus on practical implementation, considering real-world constraints and challenges specific to industrial IoT deployments. This ensures that our proposed solution is not only theoretically sound but also feasible in actual industrial settings.

The structure of this paper is as follows: Section 2 presents the significance and contributions of this study, while Section 3 introduces the system model. The IoT transmission scheme and the proposed switching algorithm are detailed in Section 4 and Section 5, respectively. Section 6 evaluates system performance, focusing on data rate and energy efficiency, Section 7 discusses the trade-off between energy efficiency and data transmission, and Section 8 discusses the research findings.

2. Motivation and Contribution

With the increasing interest in zero-energy devices, it is time for the concept to be introduced in practical settings such as warehouses. The use of sensors and wireless

communication in large-scale warehouses and related relays provide the opportunity to explore the use of various energy harvesting strategies. We propose a hybrid switch with decision-making between ABCS and SWIPT for wireless data transfer purposes. It determines the parameters of the received data signal alongside the energy available in the battery and switches between SWIPT and ABCS to maintain continued operation.

In large-scale warehouses, the data collection sensor/robots move through the warehouse, and when the size of the warehouse increases, it is ideal to have a relay to support the transmission of the gathered data to the required destination. Our switch can be implemented as the relay, and since it operates purely through harvested energy, it can be placed per the physical requirements without constraints related to the power supply for the switch.

Considering the advances that can be achieved through the combination of SWIPT and ABCS towards performance and efficiency improvement, the contributions of this paper can be summarized as follows:

- Development of an adaptive switching algorithm that optimizes the trade-off between energy harvesting and data transmission in indoor IoT environments.
- Design of a hybrid relay system capable of seamlessly transitioning between ABCS and PS-SWIPT modes to maintain quality of service while maximizing energy efficiency.
- Comprehensive performance analysis of the proposed system in a simulated warehouse environment, demonstrating its superiority over single-mode ABCS or SWIPT systems.
- Investigation of the system's behavior under various channel conditions and distances between nodes, providing insights into its applicability in diverse industrial IoT scenarios.

3. System Model

We consider an indoor warehouse, where the source node (S) moves along a preassigned pathway, and the relay switch (R) is located at the highest reachable point inside the warehouse, where a direct line-of-sight (LoS) path can be made with S. The destination node (D) is an IoT receiver that processes the data for the required information. We consider that this system is implemented in a standard warehouse with boxes stored and we assume that this consideration allows for a better visualization of the real-world warehouse environment within the simulation.

It is assumed that the data transmission occurs from S to R, and R switches to either PS-SWIPT or ABCS based on received signal parameters. There is no direct link from S to D due to severe path loss and obstacles (which would affect the assumption of the simulation modeling the real-world scenario). For the scope of this system, we consider that there is no data processing occurring at R, and all processing functions are carried out once the signal is received at D [26]. The warehouse environment is shown in Figure 1.

3.1. Line-of-Sight Probability

It is assumed that the sensor moves on a preassigned path and would transmit data to R at random time intervals. Thus, the probability of an LoS existing for the transmission would depend on the location of the sensor at a given time t_1 and the height of the boxes stored in the path of the signal.

For the calculation of LoS probability, the following assumptions related to the physical structure of the warehouse are made:

- The stacks are huge and thick and can be assumed as walls;
- The stacks are placed in equal distances;
- The roof is of fixed height h.

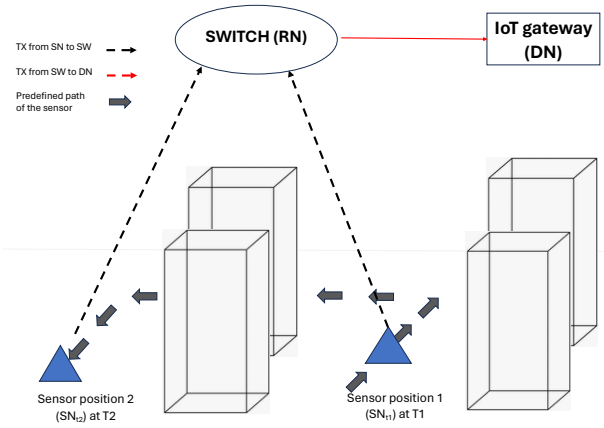


Figure 1. Structure of the indoor warehouse environment.

The warehouse is considered to be of size C_i with dimensions $W_i(m) \times L_i(m) \times H_i(m)$, and it is assumed that the space between each stack is a rectangular cavity and the system can be divided into N equal rectangular cavities, with area S_i. At a given time, if S and R are located in the same rectangular cavity, the link is an LoS link. The transmission path from S through relay node (RN) to the destination node (DN) is shown in Figure 2.

For a link of distance d_{SR}, the horizontal distance between S and R is denoted as d', where $d' = \sqrt{d_{SR}^2 - h^2}$, and the angle of d' is expressed as θ. x and y are the distances from the mid-point of d' to the sides of lengths $L(m)$ and $W(m)$, respectively. The values of x, y, and θ are independent, and if U denotes the uniform distribution, $x \sim U(0, \frac{L_i}{2})$, $y \sim U(0, \frac{W_i}{2})$, and $\theta \sim U(0, \frac{\pi}{2})$, the joint probability density function (PDF) $f(x, y, \theta)$ is given as follows:

$$f(x,y,\theta) = \begin{cases} \frac{8}{L_i M_i \pi}, & (x,y,\theta) \in A \\ 0, & \text{else} \end{cases}$$

where $A = \{(0 \le x < \frac{L_i}{2}) \cap (0 \le y < \frac{W_i}{2}) \cap (0 \le \theta < \frac{\pi}{2})\}$.

For an LoS link to exist in a given rectangular box, the following condition has to be met:

$$\left(x > \frac{d'cos\theta}{2}\right) \cap \left(y > \frac{d'sin\theta}{2}\right).$$

As presented in [27], the LoS probability changes with the horizontal length of the link d', and for simplicity, we assume that in the presented system, this length is always less than L_i. Then, the LoS probability for a single rectangular space is given as follows:

$$P_{LoS}(d) = \begin{cases} \frac{d^2 - 2d(L_i + M_i) + L_i M_i \pi}{L_i M_i \pi}, & \text{if } d < M_i \\ \frac{-L_i^2 + 2dM_i(\sqrt{1-(L_i/d)^2} - 1)}{L_i M_i \pi} + \frac{2L_i M_i \arcsin(L_i/d)}{L_i M_i \pi}, & \text{if } M_i \le d < L_i \\ 0, & \text{otherwise} \end{cases} \quad (1)$$

In the complete warehouse with N rectangular spaces, the LoS probability can be found using Equation (2),

$$P_{LoS}(d') = \sum_{i=1}^{N} \frac{S_i}{\sum_{i=1}^{N} S_i} P_{i,LoS}(d'). \quad (2)$$

Thus, based on P_{LoS}, the Rician factor can be expressed as follows:

$$K = \frac{P_{i,LoS}(d')}{1 - P_{i,LoS}(d')}. \tag{3}$$

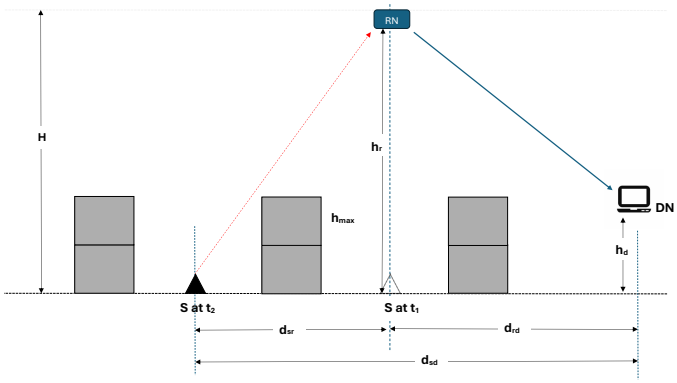


Figure 2. Transmission path with S to RN (in red), and RN to DN (in blue) with the positions of each node. S node changes location with time.

3.2. Channel Gain

The system operates in a Rician fading channel, and the PDF for the channel gain can be calculated using Equation (4), where A^2 is the power of the LoS components and $2\sigma^2$ is the power of the NLoS components.

$$p_R(r) = \frac{r}{\sigma^2} \cdot \exp\left(-\frac{r^2 + A^2}{2\sigma^2}\right) \cdot I_0\left(\frac{Ar}{\sigma^2}\right) \tag{4}$$

This can also be written using the Rician factor K as [28]:

$$K = \frac{A^2}{2\sigma^2}. \tag{5}$$

The average envelope of the distribution for R in Equation (4) can be given as $E\{R^2\} = \overline{R} = A^2 + 2\sigma^2$; hence, we can rewrite the PDF for the channel distribution as follows:

$$P_R(r) = \frac{2r(K+1)}{\overline{R}} \exp\left(-K - \frac{r^2(K+1)}{\overline{R}}\right) I_0\left(2r\sqrt{\frac{K(K+1)}{\overline{R}}}\right) \tag{6}$$

4. Transmission Through the Switch

Transmission from the switch to the destination occurs either using SWIPT or ABCS, depending on the energy requirements of the switch and the algorithm proposed in Section 5. We assume that the system operates under a normal transmission network with packet transmission from the S to R node and from the R to D node. It adapts BPSK modulation for SWIPT-based operation.

The transmission power requirements and energy harvesting capabilities differ significantly between SWIPT and ABCS modes. SWIPT requires higher transmission power but offers simultaneous energy harvesting capability, while ABCS provides energy-efficient transmission through signal reflection but without energy harvesting capability. This fundamental difference in power characteristics plays a crucial role in the switch's operation and mode selection.

4.1. SWIPT-Based Transmission

If the switch selects SWIPT, we consider that the system adapts BPSK modulation, with AWGN noise of 0 mean and variance σ^2.

$$y_{SR}(t) = \sqrt{\frac{P_{SR}^t}{d_{SR}^m}} h.x(t) + n_{SR}(t).$$

The system adapts a PS ratio of ρ and the signal components allocated for EH and ID are given as $y_{SR}^{EH} = (1-\rho)y_{SR}(t)$ and $y_{SR}^{ID} = \rho y_{SR}(t)$, respectively.

The SNR of the ID signal at R can be given as:

$$\gamma_{R_{SWIPT}} = \frac{\rho P_{SR}^t |h_{SR}|^2}{d_{SR}^m \sigma_{SR}^2}. \tag{7}$$

And the SNR for the signal received at D for SWIPT mode transmission can be given using

$$\gamma_{D_{SWIPT}} = \frac{\rho P_{SR}^t |h_{SR}|^2 |h_{RD}|^2}{d_{SR}^m d_{RD}^m \sigma_{SR}^2 \sigma_{RD}^2}. \tag{8}$$

With linear EH, the amount of energy harvested with the allocated signal component at R can be given as Equation (9),

$$E_{EH} = \frac{\eta(1-\rho) P_{SR}^t |h_{SR}|^2}{d_{SR}^m}. \tag{9}$$

The energy harvesting efficiency η significantly impacts the overall power management of the system. When operating in SWIPT mode, the harvested energy must exceed the power required for transmission (P_t) to maintain sustainable operation. The power splitting ratio ρ creates a direct trade-off between energy harvesting and data transmission capabilities—a higher ρ improves the data rate but reduces the harvested energy, while a lower ρ prioritizes energy harvesting at the cost of a reduced data rate.

4.2. ABCS-Based Transmission

If the switch selects ABCS mode, it operates as a backscatter tag, and the received signal $y_{SR}(t)$ is reflected to D, and the system adapts a simple OOK modulation technique. The amount of reflection depends on the reflection coefficient α:

$$\alpha = \frac{Z_l - Z_s*}{Z_l + Z_s} = Ae^{j\psi},$$

where $A \in [0, 1]$ is the modulus of the reflection coefficient, and ψ is the phase.

When $y_{SR}(t)$ is the signal received at R, the signal backscattered to D can be given as follows:

$$\begin{aligned} y_{RD}(t) &= \alpha y_{SR}(t) \\ &= \alpha \sqrt{\frac{P_{SR} P_{RD}}{d_{SR}^m d_{RD}^m}} h_{SR} h_{RD} x(t) + n(t) \end{aligned}$$

The switch is considered to have very little modulation; therefore, we can neglect the thermal noise from the backscatter tag [29].

The SNR of the received signal at D in ABCS mode is given as follows:

$$\gamma_{D_{ABCS}} = \frac{A^2 P_{SR} P_{RD} |h_{SR}|^2 |h_{RD}|^2}{d_{SR}^m d_{RD}^m \sigma_{SR}^2 \sigma_{RD}^2} \tag{10}$$

The power consumption of ABCS mode is primarily determined by the circuit power (P_{ckt}) required for reflection operations, which is significantly lower than SWIPT's transmission power requirements. The reflection coefficient α affects both the power consumption and the backscattered signal strength—higher values of α increase the reflected signal strength but also slightly increase power consumption. This makes ABCS particularly suitable for scenarios where energy availability is limited but maintaining communication links is crucial.

5. Operation of the Switch

5.1. Basic Circuitry of the Switch

For the implementation of the switch, we consider standard power harvesting and transmission specifications suitable for indoor IoT environments. The RF energy harvester is designed to operate with typical indoor ambient RF power density levels. The harvesting antenna's aperture size is selected to maintain reasonable harvesting efficiency while being practical for warehouse deployment. For power transmission, we utilize standard omnidirectional antennas operating at industrial IoT frequencies, suitable for indoor environments with multiple reflections. The transmission circuit is designed to operate within standard indoor wireless transmission power limits.

In SWIPT mode, the power harvesting circuit employs a standard rectenna configuration with a matching network designed for optimal power transfer at the operating frequency. For ABCS operation, the backscatter antenna is designed with a load impedance that can be switched between two states to achieve amplitude shift keying modulation. The reflection coefficient α is set as indicated in Table 1, which provides a balance between reflection efficiency and power consumption.

Table 1. Simulation parameters.

Parameter	Value
Length of the warehouse space in meters (L)	6
Width of the warehouse space in meters (M)	6
Height of R in meters	5
Height of D in meters	2
R position in the x,y plane	(3.5, 3.5)
D position in the x,y plane	(L, M)
P_t (transmission power)	20
pathloss exponent (m)	2
ρ (power splitting ratio for SWIPT)	0.8
σ_{SR}, σ_{RD}	0.5
A (reflection coefficient for ABCS)	0.5
Hysteresis factor	0.05
Minimum data rate threshold	10
Minimum energy harvesting threshold	10

5.2. Switch Algorithm

Selection between the two available transmission nodes in the switch is performed based on the parameters of the received signal $Y_{SR}(t)$, and the proposed algorithm for the selection between ABCS and SWIPT is given in Algorithm 1.

Algorithm 1 Decision-making algorithm for hybrid switch with ABCS and SWIPT

Initialize:
$best_scheme \leftarrow \emptyset$
$max_data_rate \leftarrow 0$
$hysteresis_factor \leftarrow HF$
$min_data_rate_threshold \leftarrow mindatarate$
$min_energy_threshold \leftarrow minenergy$
Check if SWIPT meets minimum requirements
if $data_rate_RD_SWIPT \geq min_data_rate_threshold$ **and** $energy_harvested \geq min_energy_threshold$ **then**
  $best_scheme \leftarrow$ SWIPT
  $max_data_rate \leftarrow data_rate_RD_SWIPT$
end if
Check if ABCS meets minimum requirements
if $data_rate_RD_ABCS \geq min_data_rate_threshold$ **then**
  if $data_rate_RD_ABCS > max_data_rate \times (1 + hysteresis_factor)$ **then**
    $best_scheme \leftarrow$ ABCS
    $max_data_rate \leftarrow data_rate_RD_ABCS$
  end if
end if
If neither scheme meets minimum requirements, choose the better one
if $best_scheme = \emptyset$ **then**
  if $data_rate_RD_SWIPT > data_rate_RD_ABCS$ **then**
    $best_scheme \leftarrow$ SWIPT
  else
    $best_scheme \leftarrow$ ABCS
  end if
end if
Tie-breaking mechanism
if $|data_rate_RD_SWIPT - data_rate_RD_ABCS| < 1 \times 10^{-6}$ **then**
  if $energy_harvested \geq min_energy_threshold$ **then**
    $best_scheme \leftarrow$ SWIPT ▷ Prefer SWIPT if energy harvesting is sufficient
  else
    $best_scheme \leftarrow$ ABCS
  end if
end if
Additional check for energy requirement in SWIPT
if $best_scheme =$ SWIPT **then**
  $energy_required_for_transmission \leftarrow \frac{1}{avg_h_RD} \times path_loss_RD$
  if $energy_harvested < energy_required_for_transmission$ **then**
    $best_scheme \leftarrow$ ABCS
  end if
end if

The algorithm first evaluates if SWIPT meets the minimum requirements for both data rate and energy harvesting. If these conditions are met, SWIPT is initially selected. It then assesses ABCS, choosing it if it meets the minimum data rate threshold and offers a significant improvement over SWIPT, accounting for a hysteresis factor to prevent frequent switching (The hysteresis factor allows a practical difference to be maintained when selecting between ABCS and SWIPT. Here, ABCS needs to outperform SWIPT by a factor (HF) determined by the user if both meet the minimum conditions.) In cases where neither

scheme meets the minimum requirements, the algorithm defaults to the one with a higher data rate.

A tie-breaking mechanism is implemented for scenarios where SWIPT and ABCS data rates are nearly identical, preferring SWIPT if sufficient energy can be harvested. As a final check, if SWIPT is selected, the algorithm verifies that the harvested energy is adequate for transmission, switching to ABCS if this condition is not met. This approach ensures that the selected scheme is not only optimal in terms of data rate but also feasible from an energy perspective, providing a robust and efficient solution for the hybrid switch operation.

The logic flow of the algorithm is shown in the flowchart given in Figure 3 below. The algorithm evaluates the data rate that can be achieved through SWIPT and ABCS. In cases of similar data rates that do not meet the minimum threshold, it opts to consider the better data rate achievable between SWIPT and ABCS. As can be seen from the flowchart, the algorithm pays higher attention when selecting SWIPT due to the higher energy requirement for transmission through SWIPT. For specific zero-energy implementations, the use of a less energy-consuming method is preferred; therefore, the energy consumed by the selected scheme is considered thoroughly through the switch.

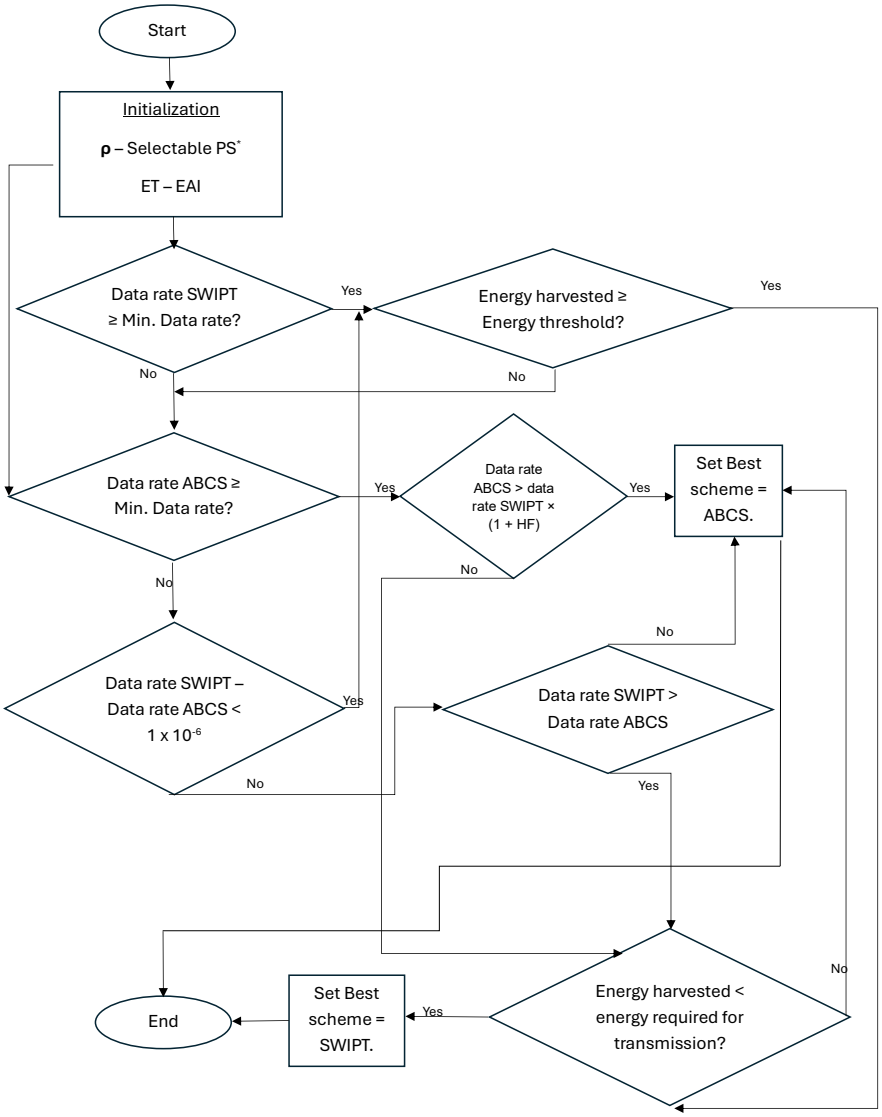


Figure 3. Operational flowchart for the proposed algorithm. * Here, value of PS changes based on the value assigned by the selectable PS algorithm, and PS selection algorithm operates before the switching algorithm.

The data rate and the energy harvesting thresholds are values which entirely depend on the environmental conditions and the operational conditions expected by the users. The algorithm, when implemented in the switch, can be initialized with the performance expected by the user. The data rate requirement in specific IoT networks change, and in industrial settings, a higher focus may be given to energy harvesting rather than the data rate. The determination of parameters for data rate and energy are associated with the transmission environment (availability of a strong LoS), and the required freshness of data at the D node. For the scope of this paper, we assume that PS ratio optimization mechanisms available in the present literature are utilized directly [30–32]. The initialization of the energy threshold (ET) and the PS ratio are automated within the switch, allowing for less interference from the users. We assume that the PS ratio is initialized using a selectable PS optimization approach, which allows the users to allow the algorithm to determine the required PS ratio [33]. For the ET, it is assumed that an energy aware interface (EAI) is utilized [34]. This approach enhances the automation of the switch and reduces the manual involvement within the overall operation. This allows the system to be operated based on a monitoring mechanism that considers the available amount of energy within the battery, and the energy required for the transmission from R to D nodes. Based on the values obtained through the EAI, the system is capable of monitoring the energy availability of the switch and thereby updating the system about the required amount of energy.

The HF represents the priority balance between EH and information transmission in the system. Expressed as a percentage, HF can be set to a lower value when neither EH nor information transmission requires precedence. However, the value needs to be adjusted based on the relative importance given to either energy harvesting or data transmission requirements in specific applications. For instance, in scenarios where energy harvesting is critical, a higher HF would ensure the system favors maintaining SWIPT operation when conditions are suitable. The HF parameter is, however, not initialized by the user or the system, and it is set as a fixed value within the switch. The calculation of HF required for the switch is based on the hardware and information requirements and is not considered within the scope of this work.

To maintain ambiguity and flexibility of the switch operations towards its environment, we allow the users to provide the required minimum data rate as an input. The switch provides a data rate scale from 1 to 3, where 1 represents the lowest data rate with a minimum PS ratio of ρ_{min} for ID, and 3 represents highest data rate with a maximum PS ratio of ρ_{max} for ID. If the user selects either of these two, the selectable PS ratio mechanism limits its range of PS towards the lowest or highest ranges, respectively. However, if the user selects scale 2, this allows the switch to automate the operation, and the data rate is considered based on the PS ratio obtained by the selectable algorithm and EAI, while thresholds for the minimum and maximum operations are fed such that the switch would not operate on either extremes (here, the extremes are when PS ratio is modeled such that there is no ID or EH components).

Under PS-SWIPT, once the selection is performed through the switch, the system needs to consider the optimal PS ratio for switching between EH and ID. Under the operational conditions of the switch, the selection for SWIPT is made if and only if the required conditions are met, and under a fixed environment, it can be assumed that the conditions at which the switch selects SWIPT are similar [35]. Thus, a fixed PS ratio is implemented for the switch, and the initialization of the ratio is to be performed by the user based on the specific environment under which it is operated. For the scope of this paper, we consider that PS ratio optimization mechanisms available in the present literature can be directly adapted [30–32]. The PS ratio is to be selected at the initialization stage of the system and though this parameter is not required by the algorithm (which is implemented to

determine between ABCS and SWIPT based on the received signal conditions and expected performance) , it is required by the switch under operation based on the SWIPT mechanism.

The algorithm operates by utilizing physical layer parameters, specifically the received signal power and CSI, to determine the optimal transmission mode. During the relay-to-destination (R to D) transmission phase, the system employs standard packet transmission protocols. The algorithm's sole function is mode selection between SWIPT and ABCS, while actual data transmission follows conventional IoT network protocols. The security and privacy of the switch and the associated transmission network is considered to be based on IoT network security features.

Gateways between different nodes can be provided with specific security features, and shielding practices such as end-to-end encryption algorithms can also be considered [36]. However, this may compromise the computational complexity and the overall energy requirement of the switch, which would therefore require a careful consideration of the ideal data security and privacy enhancement technique adapted in the switch.

5.3. Complexity Analysis of the Algorithm

The number of operations of the algorithm $T(n)$ can be given in terms of the input size n, and it is bounded by a constant c for all $n \geq n_0$, where $n_0 \in \mathbb{Z} \geq 0$. Here, n is defined as the number of input parameters considered for initialization and $T(n)$ is the number of operations performed.

We can express $T(n)$ as follows:

$$T(n) = a_1 + a_2 + a_3 + a_4 + a_5 + a_6, \tag{11}$$

where a_1, a_2, a_3, a_4, a_5, and a_6 are the numbers of operations for initialization, checking SWIPT requirements, checking ABCS requirements, choosing between schemes if neither meets the requirements, tie-breaking mechanism, and additional check for energy requirement in SWIPT, respectively. These operations $(a_1, a_2, \ldots, a_6)$ consist of a fixed number of functions, regardless of the input size n; therefore, we can consider each a_i as a constant.

Let $c = a_1 + a_2 + a_3 + a_4 + a_5 + a_6$. Thus, $T(n) = c$ for all $n \geq 0$. By the definition of Big O notation, an algorithm is $O(1)$ if there exist positive constants c and n_0 such that $T(n) \leq c$ for all $n \geq n_0$. In the presented algorithm, this inequality holds for all $n \geq 0$, with c being the sum of our constant terms, thus resulting in $T(n) \in O(1)$.

6. Simulation Results

This section presents the simulation results obtained to validate the theoretical derivations, and to determine the requirement of the SWIPT- and ABCS-enabled hybrid switch as per the values presented in Table 1.

It is considered that S moves through the warehouse floor and transmits data to R while being at specific locations given in Figure 4. For simplicity, we assume that all the positions presented in the figure are within the warehouse floor and no walls or other barriers are present in these specific locations. Also, it is assumed that S stays stationary while transmitting, and once the transmission is completed, it moves to the next position.

The following simulations of the system are conducted with respect to the x, y coordinates of these transmission points. The results are demonstrated with variations in x coordinates along specific y coordinates, and for each transmission node, for a better comparison, we consider transmission using an AF relay model without any EH process, transmission using ABCS alone with EH, transmission using SWIPT-enabled relay scheme with EH, and transmission using the proposed algorithm with EH.

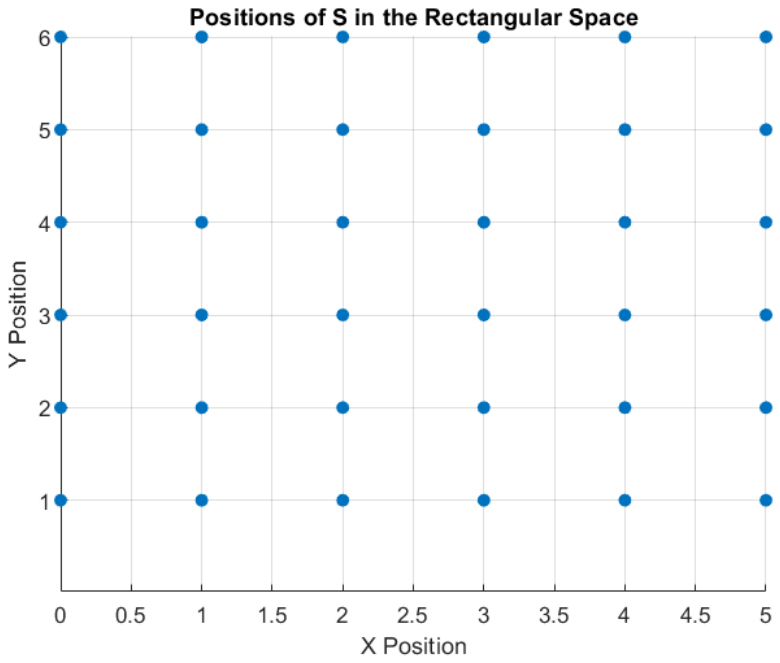


Figure 4. Transmission points of *S* to *R* within the warehouse floor (each dot on the plane shows a transmission point).

6.1. Transmission Through an AF Relay Scheme

For comparison, we consider the operation of the system if *R* were an amplify-and-forward relay without any energy harvesting scheme. The SNR of the system for an AF relay scheme is shown in Figure 5 and the drainage of battery for a single cycle (The complete transmission of data from *S* to *R*, covering all the transmission points identified in Figure 4, is referred to as a single cycle. The system is assumed to cover one complete cycle from $(0, 1)$ to (5, 6) by moving along the y-axes and then return to the initial position while completing the second transmission cycle) of operation is shown in Figure 6.

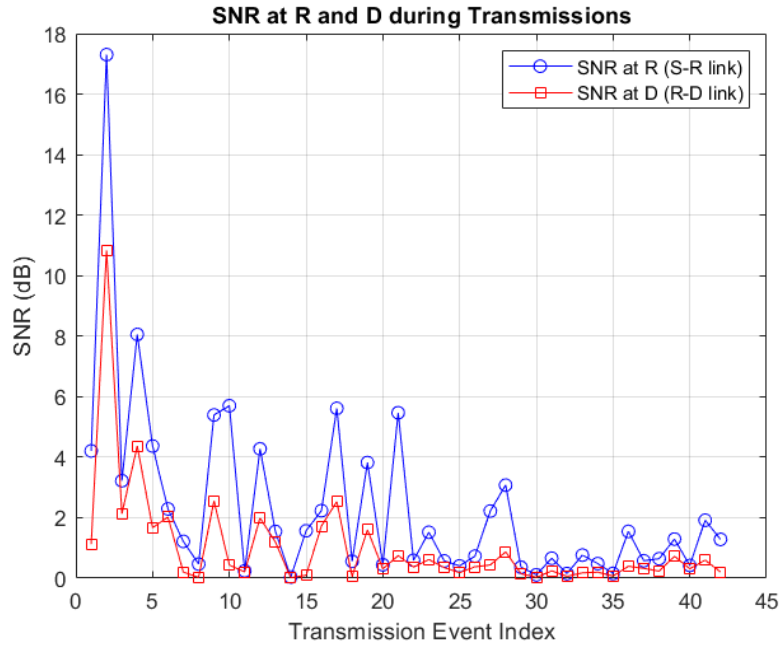


Figure 5. SNR at *R* and *D* when the switch is implemented with an AF Relay system.

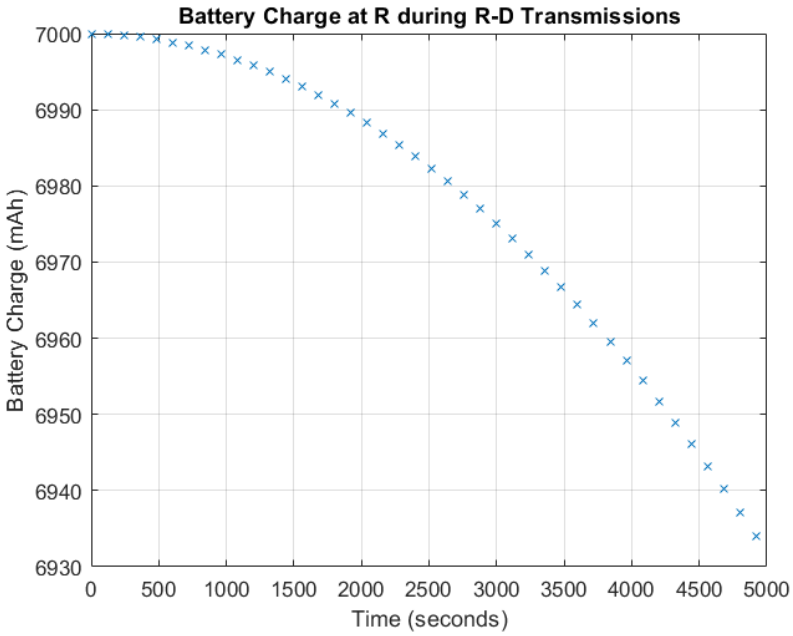


Figure 6. Battery discharge performance during a single cycle of operation with AF relay-based transmission.

Through an AF relay-based transmission, the system would be capable of maintaining a higher SNR at D through the amplification of the signal, yet the energy requirement for amplification process once again creates considerable issues when maintaining system performance.

The battery drainage model of a Li-ion battery is considered for the study, and within an approximate 5000 s of transmission, it can be seen that the battery drains approximately by 70 mAh. If the system were to transmit continuously, this drainage would create a considerable issue in maintaining the battery charge, since the system shows a drainage of 0.72% per hour. In the case of the proposed system, the battery losses for a single cycle as shown in Figure 6 is considerably low since the transmission takes place within a short time period. This massive drainage occurring through a very short time period also lays the foundation for the requirement of adapting energy harvesting mechanisms.

The battery performance of the AF relay system demonstrates the inefficiency of using a simple relay model-based transmission scheme within the indoor environment, especially when major focus is put on energy efficiency and zero-energy device implementation, as the requirements of continuing operation with limited battery replacement is hindered in this case.

6.2. Transmission Using a SWIPT-Enabled Relay

We now consider the operation of R if it were to operate solely through SWIPT. With SWIPT, the system is capable of harvesting energy while transmitting data to D and addresses one of the main issues that was identified in the AF-based relay system discussed earlier.

The SNR achieved at D when using SWIPT is presented in Figure 7, and the energy harvesting capability when using SWIPT exclusively at the relay node for different source positions in the warehouse plane is shown in Figure 8. The results reveal that energy harvesting performance varies significantly with source location, achieving maximum efficiency when the source node is positioned closer to the relay. This spatial dependency of energy harvesting is particularly evident in the central regions of the warehouse (around the relay position at (3.5, 3.5)), where harvested energy levels reach their peak values. However, as the source moves towards the warehouse boundaries, especially at higher y

coordinates, the harvesting efficiency decreases substantially due to increased path loss and potential signal degradation. This pattern highlights a key limitation of relying solely on SWIPT—while it provides excellent energy harvesting capabilities under favorable conditions, its performance becomes suboptimal when the source–relay distance increases or when channel conditions deteriorate.

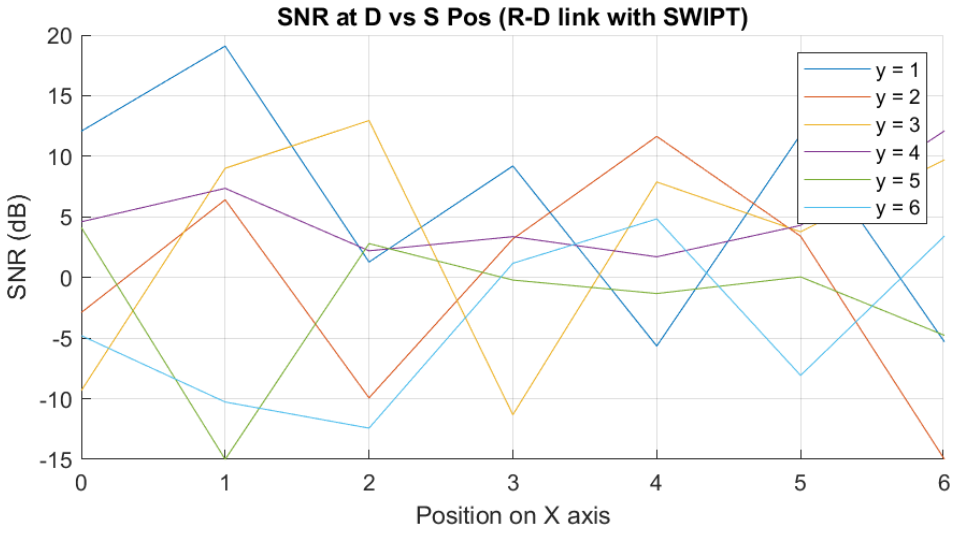


Figure 7. Variation of SNR at *D* node when when transmitting with SWIPT from *R* to *D*.

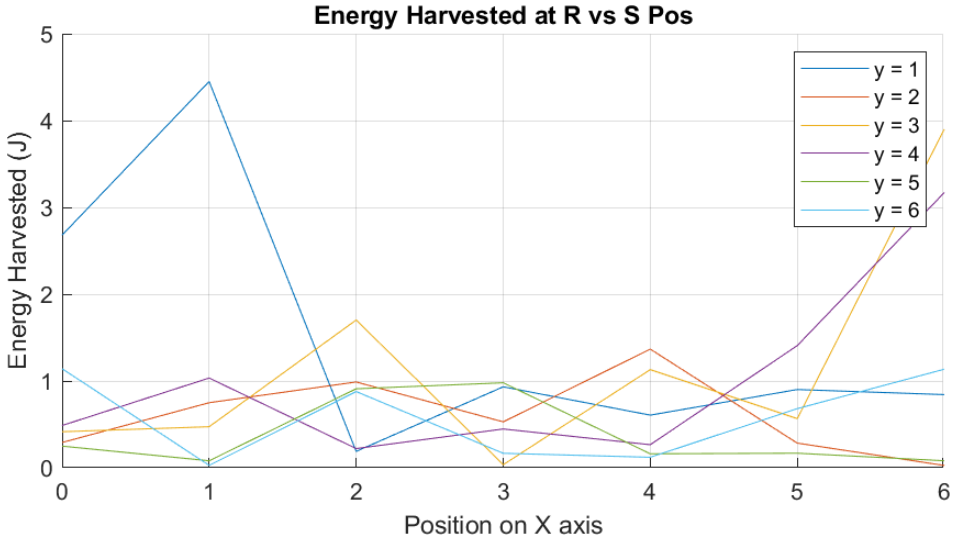


Figure 8. Variation of Energy harvested at *R* when using SWIPT for different S locations within the warehouse.

The energy harvested at *R* with the SWIPT system allows for a considerable increment in the system's energy gain. With the movements of *S*, the amount of energy harvested varies, but is still capable of maintaining appreciable performance especially when in locations where the *S* node is closer to the *R* node.

6.3. Transmission Using an ABCS-Enabled Relay

When using a system that operates entirely through the ABCS, the SNR of the signals received at *D* for the transmission within the warehouse is given in Figure 9.

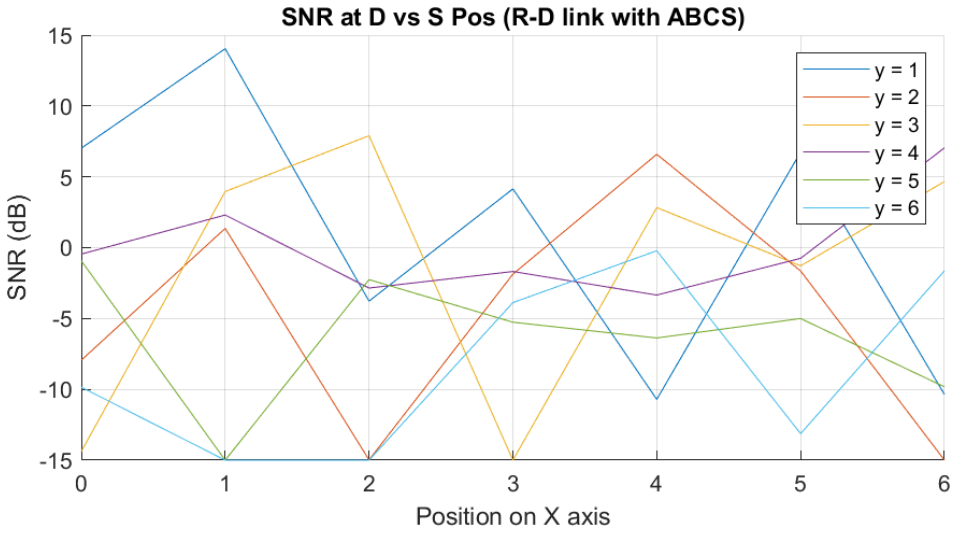


Figure 9. SNR at *D* if the relay used ABCS for transmission at specific S locations of x and y coordinates in the warehouse plane given in Figure 4.

Compared to the performance of SWIPT, the SNR performance of ABCS is lower, and the maximum SNR achieved for the R-D link is approximately 14 dB. High-SNR points are visible at critical transmission points near the relay when SWIPT is implemented as the selected methodology in the relay, as can be seen from Figure 7. This is one of the inherent features of ABCS, since the transmission process relies on the reflection of the received signal, and the reflection coefficient plays an important role in the received signal SNR.

The lower ranges of SNR for both SWIPT and ABCS take almost equal values, and the performance of the two systems at these regions can be evaluated using the energy required for transmission while maintaining an appropriate data rate. ABCS, however, provides a better opportunity when implementing low-energy transmission, in scenarios where energy harvesting is not possible.

6.4. Transmission Using Proposed Algorithm

Performance of the proposed algorithm is evaluated in a two-fold approach—the energy harvested at the switch, and the QoS achieved at the destination. This evaluation allows us to determine the superiority of the switch with respect to the existing schemes.

6.4.1. QoS at *D*

The SNR achieved at *D* for specific x and y locations in the warehouse plane is shown in Figure 10. The algorithm operates by maintaining a balance between the received signal conditions to achieve a better data rate as well as to ensure that the energy consumption through the system is maintained appropriately. We consider that an initially fully charged battery is used in the system; thus, the algorithm does not have any conditions for the initial selections, therefore providing a better opportunity to maintain higher performance.

As can be seen from the results, the SWIPT scheme was selected in most cases, and ABCS was selected only in scenarios where the SNR was considerably low. Since *S* moves across the warehouse floor, it is evident that specific locations that are further away from *R* result in considerably lower SNR, and in such instances, the additional requirement of the ability to harvest sufficient energy for transmission plays a major role in determining the ideal transmission scheme.

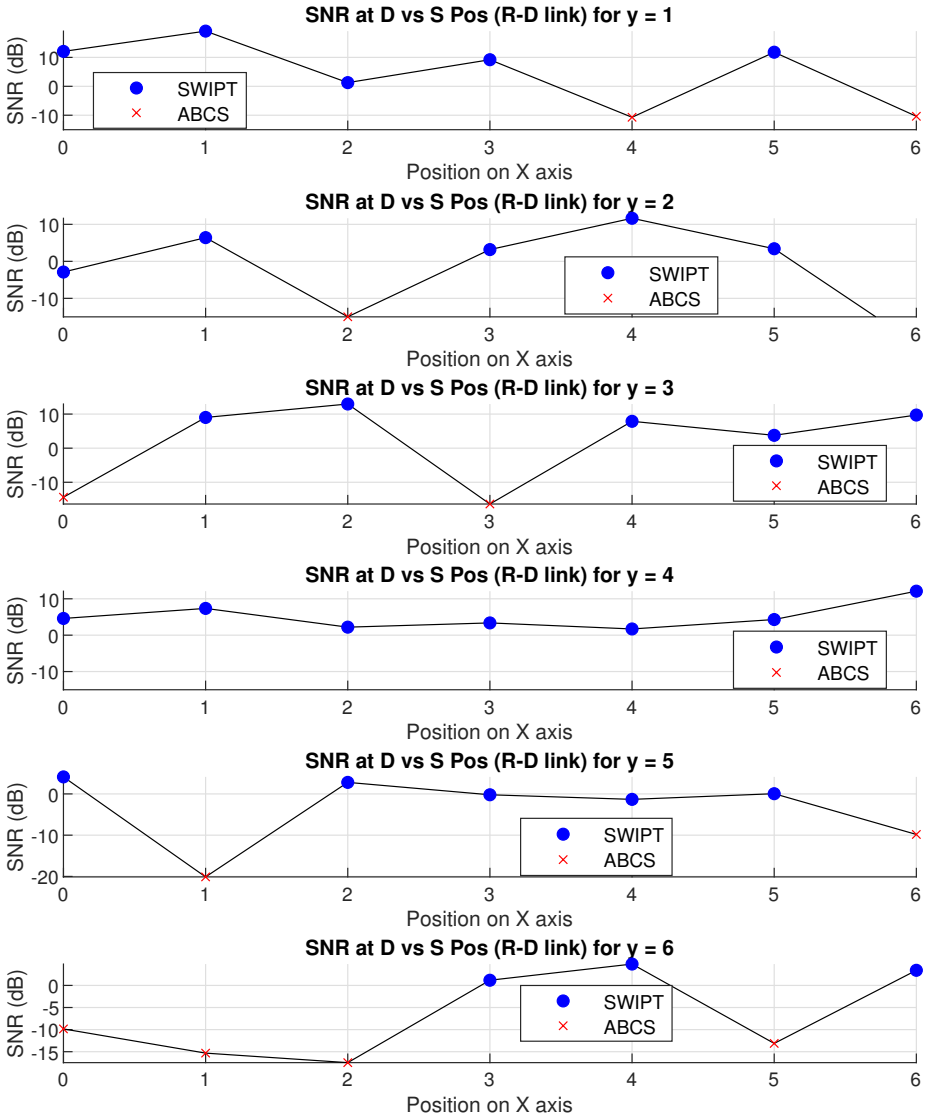


Figure 10. SNR achieved at D when using the proposed algorithm for transmission from R to D.

In instances where the SNR of the signal received at R is considerably low, the ability to harvest the required amount of energy for transmission is hindered; hence, the algorithm opts for ABCS to support energy consumption.

The highest performance is shown when S moves along the $y = 3$ and $y = 4$ axes, and this is due to the placement of R at (3.5, 3.5). Maintaining a closer distance between the $S - R$ link undoubtedly supports the transmission in the $R - D$ link; however, only the furthermost points of the warehouse show considerably lower SNR values. Better performances can be seen at the $y = 1$ and $y = 2$ axes; however, the lowest performance is seen at the $y = 6$ axis.

The drastic decrease in performance, which would be inevitable if the system were to adopt either ABCS or SWIPT, as well as the massive battery power consumption if the system were to rely on another relay model as shown, is significantly mitigated while providing better performance through the selection between the provided transmission schemes.

6.4.2. Energy Harvesting Performance at R

Energy harvesting is conducted only when the switch selects SWIPT mode for transmission. The selection is performed based on the amount of energy required for transmission and the amount of energy harvestable based on the received signal.

Figure 11 illustrates the comparative energy profiles when using the proposed hybrid switching algorithm, showing three critical parameters: energy harvested through SWIPT, periods of no harvesting during ABCS operation, and the required battery contribution. The results are presented across different y coordinates ($y = 1$ to $y = 6$) to demonstrate the system's adaptive behavior throughout the warehouse space. In locations where SWIPT is selected (primarily $y = 1$ to $y = 4$), the harvested energy often exceeds 2 J, indicating efficient energy capture that minimizes battery dependency. Particularly noteworthy is the algorithm's intelligent switching behavior—when harvested energy becomes insufficient for SWIPT operation (as seen in the $y = 5$ and $y = 6$ positions), the system automatically switches to ABCS mode, requiring minimal battery contribution while maintaining communication capability. The algorithm chooses SWIPT as the transmission scheme when the required energy for transmission is considerably lower, and only in instances where the system is capable of harvesting energy greater than required. The battery contribution in instances where SWIPT is selected is, therefore, almost zero, and only in cases where ABCS is selected does the battery have to provide a higher power for transmission. This allows us to effectively utilize battery energy and to ensure that the system has the capability to maintain transmission in a self-sustaining manner.

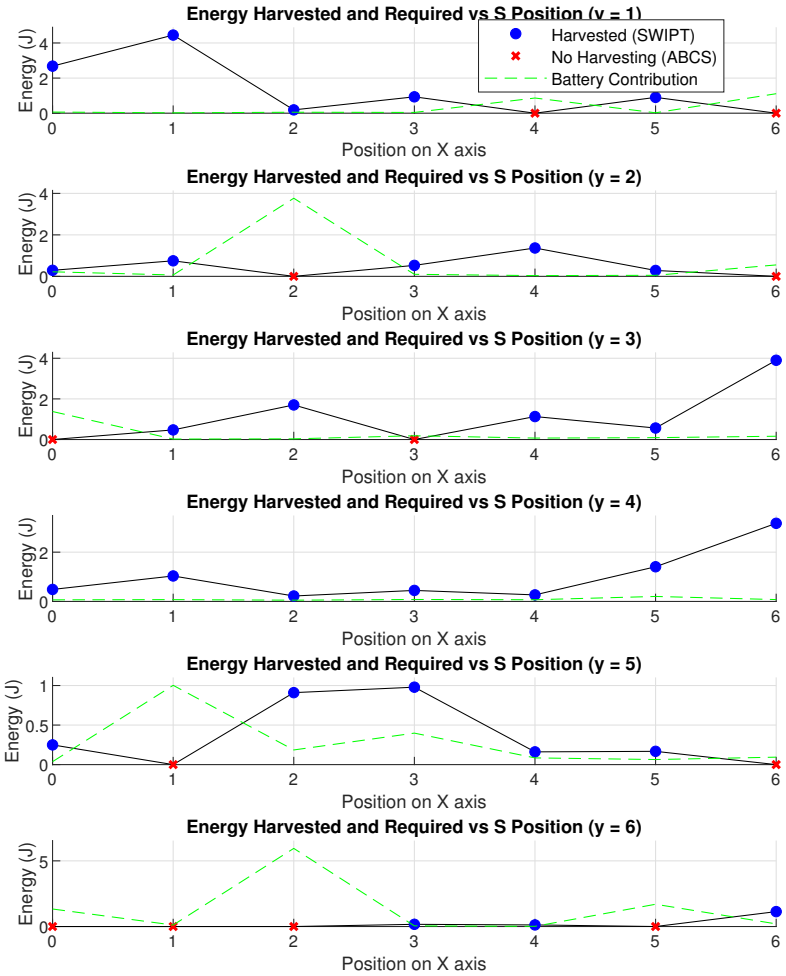


Figure 11. Variation of Energy harvested at R when using the proposed algorithm for transmission at R node.

In cases where ABCS is selected, it can be seen that the system does not harvest any energy, yet the requirement of energy for transmission is considerably high. This can be associated with the low quality of the received signal, which thereby requires higher

transmission power to maintain signal quality. The system focuses not only on energy harvesting conditions but also on the QoS; therefore, to maintain the data rate at the expected level, the system has to provide a higher transmission power. In such instances, the system opts to utilize the energy inherently available in the battery, thereby ensuring that the QoS at D is not compromised. The least amount of harvested energy is seen when the sensor is at the farthest position from the switch. Since the transmission occurs in an indoor environment, this increase in distance increases the path loss and fading, thereby calling for adaptations to maintain expected performance standards. The inefficiency of operating solely with a SWIPT-enabled system under low signal conditions is thereby addressed by the proposed system.

The complementary nature of Figures 8 and 11 demonstrate the advantages of the hybrid approach over single-mode operation. While Figure 8 shows the limitations of pure SWIPT operation, Figure 8 reveals how the hybrid system overcomes these limitations by dynamically switching between modes based on energy availability and requirements. This adaptive behavior ensures consistent performance across varied warehouse locations while optimizing energy utilization.

6.5. Power Management Analysis

The power management capability of the proposed switch can be analyzed through two key aspects: power harvesting efficiency and transmission power requirements. As demonstrated in Figure 8, SWIPT mode achieves optimal energy harvesting when the source node is positioned near the relay, with harvesting efficiency decreasing as the source–relay distance increases. This spatial dependency of energy harvesting directly influences the switch's mode selection decision.

Figure 11 further illustrates the system's power management strategy across different source locations. When operating in optimal positions (y = 1 to y = 4), the switch predominantly utilizes SWIPT mode, harvesting sufficient energy (often exceeding 2 J) to support transmission requirements. However, in challenging positions (y = 5 and y = 6), where harvesting efficiency decreases, the switch intelligently transitions to ABCS mode to maintain communication while minimizing power consumption.

The relationship between harvested power and transmission requirements can be observed through the algorithm's decision-making process. When the energy harvested through SWIPT meets the minimum energy threshold requirement, and the data rate conditions are satisfied, the switch maintains SWIPT operation. In scenarios where these conditions cannot be met, particularly in positions farther from the relay, the switch transitions to ABCS mode. This transition reflects the system's ability to adapt its power management strategy based on real-time conditions, ensuring efficient operation across varied warehouse locations while maintaining communication capability.

7. Trade-off Between Energy Efficiency and Data Transmission

The proposed hybrid switch and its associated mechanism achieve a balance between energy efficiency and data transmission rate through dynamic adaptation based on the received signal conditions, which changes continuously, at the position of the S node. The switching decision considers three key factors that determine the optimal operation mode selection for various application scenarios and conditions. In the simulation results, the varying environment is modeled using the movement of the S node throughout the warehouse floor, thereby creating different LoS and NLoS conditions with varied signal powers at each position.

In situations where energy preservation is critical, such as sensors placed in hard-to-reach locations, the switch favors ABCS when the received signal strength is adequate, as it

consumes minimal power while maintaining basic connectivity. This is showcased through the simulation results by the switch opting for ABCS in scenarios where the received power is low. Conversely, in applications requiring frequent data updates, like real-time monitoring, the switch preferentially selects SWIPT when channel conditions permit, as it offers higher data rates.

Under strong LoS conditions with a direct path between nodes, SWIPT mode achieves data rates up to

$$R_{\text{SWIPT}} = \min(\log_2(1+\gamma_s), \log_2(1+\gamma_d)), \tag{12}$$

while energy harvesting efficiency is given by

$$\eta_{\text{eh}} = P_{\text{rx}} \cdot \rho, \tag{13}$$

where γ_s and γ_d are the SNRs at the relay and destination, respectively, P_{rx} is the received power, and ρ is the power splitting ratio. In contrast, under poor LoS conditions with significant path loss, ABCS mode maintains connectivity with the following data rate:

$$R_{\text{ABCS}} = \log_2(1+\gamma_b), \tag{14}$$

while consuming minimal energy ($P_c \approx P_{\text{ckt}}$), where γ_b is the backscatter SNR and P_{ckt} is circuit power consumption.

These factors allow us to determine the initialization process of the switch. To maintain the balance between energy efficiency management and data transmission, the switch considers the aspects of data rate requirement selected by the user at the initialization stage and the real-time energy requirement of the switch using the EAI. If the EAI shows that the switch has a considerable amount of energy to continue operation, higher precedence is given towards data transmission by the switch (the prioritization of data transmission over energy harvesting, unless energy harvesting takes precedence based on EAI readings, would be performed based on the user requirements provided at the switch initialization stage). However, if the EAI shows that the amount of energy is not sufficient for overall hardware functionality, the switch prioritizes energy harvesting. Thereby, a balance between energy harvesting and data transmission is obtained. Any such alterations would be adapted based on the real-time operation of the switch, which enhances operational efficiency. On the other hand, the HF parameter helps maintain balance between energy harvesting and data efficiency in all scenarios.

When considering application-specific optimization requirements, such as in indoor warehouse monitoring, periodic sensor readings typically require low data rates, thus allowing for more focus to be laid on the energy harvesting aspect of the switch. In contrast, inventory updates may demand higher throughput, necessitating greater focus on the data rate, with energy harvesting prioritized only when it does not hinder the data rate. The use of EAI and selectable PS ratio brings the opportunity to initialize the variables accordingly, thereby achieving the required performance based on the environment, since the PS ratio is selected based on the signal conditions and the EAI operates based on the hardware requirements. Further, the adaptive decision-making within the proposed algorithm originally takes place based on the received signal conditions. This allows for the decision-making algorithm proposed for the switch to be readily implementable without any further adjustments. Thus, it can be stated that the manner in which the algorithm has been developed allows it to be capable of being implemented in any environment or application without requiring changes within the algorithm, and the changes are to be made only on the parameter initialization process. However, the switch mechanism proposed

also allows it to be maintained automatically, thereby requiring very low intervention from the users.

8. Conclusions and Discussion

The proposed system adapts an integrated SWIPT and ABCS system to improve overall operational performance within an indoor environment. The main objective of the system was to develop a decision-making system that would effectively determine the choice between the two available options while maintaining better performance in terms of energy harvesting and information transmission. The integration of SWIPT and ABCS in a hybrid switch offers significant potential for energy efficiency in IoT networks deployed in warehouses. By leveraging both energy harvesting and passive communication techniques, the switch reduces dependency on external power sources and enhances operational autonomy.

The specific selection of ABCS and SWIPT for the switch was also proven suitable due to the energy harvesting limitations and performance issues that arise when the source node moves away from the relay. The ideal option in cases where the EH probability is the lowest was shown to be ABCS; thus, the results show that the usage of this scheme within the switch allows for continued transmission during the worst conditions. Simulation results show that a mutual balance between power consumption and recharging of the system is achieved through the adaptation of the hybrid mechanism.

The moderate to high SNR levels achieved by SWIPT ensure reliable data transmission, while the energy-efficient nature of ABCS provides a fallback option in challenging signal conditions. This dual approach enhances the overall robustness and reliability of data transmission in warehouse IoT networks.

The initialization mechanism in the algorithm, based on aspects such as the hysteresis factor, minimum required threshold values, and trade-off between energy harvesting and QoS, allows the switch to adopt a more practical approach.

Within the selected indoor setting, the system performance varied when the transmission distance from S to R increased. As seen from the simulation results, the proposed algorithm effectively switched between SWIPT and ABCS based on real-time parameters such as data rate requirements, energy harvesting capabilities, and SNR conditions. The switch was successful in ensuring that an appropriate amount of energy was harvested at R, complying with the requirements of transmission in the R-D link, while making sure that the quality of service maintained at D was not compromised. The adjustment of transmission power at R to address the low signal quality demonstrated the capability of the switch to address the expected performance requirements.

The main advantage of the system is the minimization of the requirement for a direct power source, or continuous battery replacement. The system, since it is capable of evaluating its own energy utilization and adjusting the transmission mode to suit the least energy-consuming methodology, offers a far longer battery life than any other energy harvesting-based or battery-powered relay.

While the simulation results demonstrate the promising performance of the proposed hybrid switch, future research will focus on experimental validation in real-world environments. This practical implementation will provide insights into the power consumption characteristics of the switch and its performance under various environmental conditions. It would be further interesting to evaluate how the system performance would change in instances where the destination node changes position as well. Such an adaptation would further hinder the performance of the system, and requirements in improvements in the proposed algorithm may be called for, in order to address the Doppler effect and distance-related issues.

While the addition of novel transmission methods to the system may be advantageous, the computational complexity of the switch would be too high, thereby requiring more power for decision-making. Thus, substituting the proposed transmission mechanisms with other suitable schemes may deem viable in certain use cases. Practical adaptations of the switch in indoor industrial environments can support the current expectations of energy efficiency, and allow us to address the requirement of zero-energy devices. This system can also be adapted in outdoor settings, where performance evaluation may be different due to differences in the fading channel and the transmission pathway. Additionally, future work will explore the adaptability of the switching algorithm under different fading environments and investigate its application in indoor 6G IoT environments, including miniature THz environments and network slicing-based transmission schemes.

Future improvements of the switch performance can be included through an addition of a feedback loop to monitor the real-time SNR of the system and to adjust the power splitting ratio and/or reflection coefficient accordingly. However, this would require a more detailed consideration on the algorithm's complexity, since this will directly affect the overall run-time and power requirement for switch operation.

This study presently considers the transmission requirements, switch operation, and other associated features. However, another predominant aspect of the transmission network that needs to be carefully considered is the security of the wireless network. Though the scope of this study is limited to the introduction of the switch, future studies need to consider aspects of data encryption within the switch. The switch can also be considered within studies exploring advanced security features such as edge devices.

Further, when considering the proposed algorithm, the objective is to determine the selection between the transmission modes, ABCS and SWIPT, in order to achieve higher energy efficiency and transmission accuracy while harvesting energy where possible. Thus, any security features to be embedded within the switch are implemented once the selection between ABCS and SWIPT has been made. The security features for the transmissions for ABCS and SWIPT modes may differ as required, thereby providing a more advanced security system.

Future research should also consider the implementation of an energy-efficient hardware unit for the switch, so that the switch requires less energy for operation. Aspects such as low-power sensors and electronics should be considered, along with the operational efficiency of the electronics associated with the switch. This would reduce the energy requirements for operation, thereby providing a better opportunity to focus on better transmission.

Based on the simulation results obtained, it can be seen that the switch performance is ideal in terms of the requirements of the indoor environment in which the switch is located, the requirements of the zero-energy devices concept, and the adaptation of SWIPT and ABCS schemes in a practical environment.

Author Contributions: Conceptualization, V.P.S., T.D.P.P. and D.N.K.J.; methodology, V.P.S., T.D.P.P. and D.N.K.J.; validation, V.P.S. and T.D.P.P.; formal analysis, V.P.S. and T.D.P.P.; investigation, V.P.S. and T.D.P.P.; resources, V.P.S., T.D.P.P. and D.N.K.J.; data curation, V.P.S. and T.D.P.P.; writing—review and editing, V.P.S., T.D.P.P. and D.N.K.J.; supervision, T.D.P.P. and D.N.K.J.; project administration, T.D.P.P. and D.N.K.J. All authors have read and agreed to the published version of the manuscript.

Funding: This work was supported, in part, by the national funds through FCT—Fundação para a Ciência e a Tecnologia—as part of the projects AIEE-UAV (No. 2022.03897.PTDC), URLLC-UAV (2023.08191.CEECIND), and COPELABS (No. UIDB/04111/2020), by the COFAC—Cooperativa de Formação e Animação Cultural, C.R.L. (University of Lusófona University), via the project PortuLight (COFAC/ILIND/COPELABS/2/2023), and by the Scheme for Promotion of Academic & Research Collaboration (SPARC), Government of India, via grant no. SPARC/2024-2025/NXTG/P3524.

Data Availability Statement: All data are available within the paper.

Conflicts of Interest: The authors declare no conflicts of interest.

References

1. Song, Y.; Yu, F.R.; Zhou, L.; Yang, X.; He, Z. Applications of the Internet of Things (IoT) in Smart Logistics: A Comprehensive Survey. *IEEE Internet Things J.* **2021**, *8*, 4250–4274. [CrossRef]
2. Sun, Z.H.; Chen, Z.; Cao, S.; Ming, X. Potential Requirements and Opportunities of Blockchain-Based Industrial IoT in Supply Chain: A Survey. *IEEE Trans. Comput. Soc. Syst.* **2022**, *9*, 1469–1483. [CrossRef]
3. Salem, R.M.M.; Saraya, M.S.; Ali-Eldin, A.M.T. An Industrial Cloud-Based IoT System for Real-Time Monitoring and Controlling of Wastewater. *IEEE Access* **2022**, *10*, 6528–6540. [CrossRef]
4. Farooq, M.S.; Abdullah, M.; Riaz, S.; Alvi, A.; Rustam, F.; Flores, M.A.L.; Galán, J.C.; Samad, M.A.; Ashraf, I. A Survey on the Role of Industrial IoT in Manufacturing for Implementation of Smart Industry. *Sensors* **2023**, *23*, 8958. [CrossRef] [PubMed]
5. Sooriarachchi, V.P.; Jayakody, D.N.K. Model for Advanced Sensor Placement in Wildfire Detection Systems. In Proceedings of the 2024 IEEE Wireless Communications and Networking Conference (WCNC), Dubai, United Arab Emirates, 21–24 April 2024; pp. 1–6. [CrossRef]
6. Mitsiou, N.A.; Papanikolaou, V.K.; Diamantoulakis, P.D.; Karagiannidis, G.K. Energy-Aware Optimization of Zero-Energy Device Networks. *IEEE Commun. Lett.* **2022**, *26*, 858–862. [CrossRef]
7. Shirvanimoghaddam, M.; Shirvanimoghaddam, K.; Abolhasani, M.M.; Farhangi, M.; Zahiri Barsari, V.; Liu, H.; Dohler, M.; Naebe, M. Towards a Green and Self-Powered Internet of Things Using Piezoelectric Energy Harvesting. *IEEE Access* **2019**, *7*, 94533–94556. [CrossRef]
8. Dibal, P.; Onwuka, E.; Zubair, S.; Nwankwo, E.; Okoh, S.; Salihu, B.; Mustaphab, H. Processor power and energy consumption estimation techniques in IoT applications: A review. *Internet Things* **2022**, *21*, 100655. [CrossRef]
9. Wang, Y.; Yang, K.; Wan, W.; Zhang, Y.; Liu, Q. Energy-Efficient Data and Energy Integrated Management Strategy for IoT Devices Based on RF Energy Harvesting. *IEEE Internet Things J.* **2021**, *8*, 13640–13651. [CrossRef]
10. Van Huynh, N.; Hoang, D.T.; Lu, X.; Niyato, D.; Wang, P.; Kim, D.I. Ambient Backscatter Communications: A Contemporary Survey. *IEEE Commun. Surv. Tutor.* **2018**, *20*, 2889–2922. [CrossRef]
11. Zargari, S.; Hakimi, A.; Rezaei, F.; Tellambura, C.; Maaref, A. Signal Detection in Ambient Backscatter Systems: Fundamentals, Methods, and Trends. *IEEE Access* **2023**, *11*, 140287–140324. [CrossRef]
12. Ponnimbaduge Perera, T.D.; Jayakody, D.N.K.; Sharma, S.K.; Chatzinotas, S.; Li, J. Simultaneous Wireless Information and Power Transfer (SWIPT): Recent Advances and Future Challenges. *IEEE Commun. Surv. Tutor.* **2018**, *20*, 264–302. [CrossRef]
13. Jiang, R.; Xiong, K.; Fan, P.; Zhang, Y.; Zhong, Z. Power Minimization in SWIPT Networks with Coexisting Power-Splitting and Time-Switching Users Under Nonlinear EH Model. *IEEE Internet Things J.* **2019**, *6*, 8853–8869. [CrossRef]
14. Chowdhury, C.R.; Mandal, C.; Misra, S. Sustainable Maintenance of Connected Dominating Set by Solar Energy Harvesting for IoT Networks. *IEEE Trans. Green Commun. Netw.* **2022**, *6*, 2115–2127. [CrossRef]
15. Saraereh, O.A.; Alsaraira, A.; Khan, I.; Choi, B.J. A Hybrid Energy Harvesting Design for On-Body Internet-of-Things (IoT) Networks. *Sensors* **2020**, *20*, 407. [CrossRef]
16. Li, X.; Teng, L.; Tang, H.; Chen, J.; Wang, H.; Liu, Y.; Fu, M.; Liang, J. ViPSN: A Vibration-Powered IoT Platform. *IEEE Internet Things J.* **2021**, *8*, 1728–1739. [CrossRef]
17. Zhuang, Y.; Li, X.; Ji, H.; Zhang, H. Exploiting Hybrid SWIPT in Ambient Backscatter Communication-Enabled Relay Networks: Optimize Power Allocation and Time Scheduling. *IEEE Internet Things J.* **2022**, *9*, 24655–24668. [CrossRef]
18. Ji, B.; Chen, Z.; Li, P.; Song, K.; Li, C.; Wang, D. Joint Optimization of SWIPT Enabled Ambient Backscatter Communication System with Multiple Antennas. In Proceedings of the 2021 9th International Symposium on Next Generation Electronics (ISNE), Changsha, China, 10–12 July 2021, pp. 1–4. [CrossRef]
19. Pereira, F.; Correia, R.; Jordão, M.; Carvalho, N.B. A Hybrid System combining SWIPT and Backscatter Techniques. In Proceedings of the 2020 IEEE Wireless Power Transfer Conference (WPTC), Seoul, Republic of Korea, 15–19 November 2020; pp. 323–326. [CrossRef]
20. Li, Y.; Cao, X.; Tang, J.; Shi, Y.; Xie, Q. Energy-Efficient Optical-Aided VLC-MIMO System with Centralised Optimal PI Strategy. *J. Light. Technol.* **2024**, 1–10. [CrossRef]
21. Choi, H.S.; Kim, D.I. Hybrid FS/PS SWIPT based Backscatter Communication for Internet of Things. In Proceedings of the 2020 International Conference on Information and Communication Technology Convergence (ICTC), Jeju, Republic of Korea, 21–23 October 2020; pp. 1786–1791. [CrossRef]
22. Nguyen, T.L.N.; Jun, J.Y.; Shin, Y. Ambient Backscattering-Enabled SWIPT Relaying System with a Nonlinear Energy Harvesting Model. *Sensors* **2020**, *20*, 4534. [CrossRef]

23. Esse, A.; Abdullah, K.; Habaebi, M.H.; Ramli, H.A.M. Dynamic Power Splitting Simultaneous Wireless Information and Power Transfer Split Receiver for Wireless Sensor Networks. *IEEE Access* **2021**, *9*, 129407–129416. [CrossRef]
24. Costanzo, A.; Masotti, D.; Paolini, G.; Schreurs, D. Evolution of SWIPT for the IoT World: Near- and Far-Field Solutions for Simultaneous Wireless Information and Power Transfer. *IEEE Microw. Mag.* **2021**, *22*, 48–59. [CrossRef]
25. Alamu, O.; Olwal, T.O.; Djouani, K. An overview of simultaneous wireless information and power transfer in massive MIMO networks: A resource allocation perspective. *Phys. Commun.* **2023**, *57*, 101983. [CrossRef]
26. Borrelli, A.; Monti, C.; Vari, M.; Mazzenga, F. Channel models for IEEE 802.11b indoor system design. In Proceedings of the 2004 IEEE International Conference on Communications (IEEE Cat. No.04CH37577), Paris, France, 20–24 June 2004; Volume 6, pp. 3701–3705. [CrossRef]
27. Zheng, H.; Zhang, J.; Li, H.; Hong, Q.; Hu, H.; Zhang, J. Exact Line-of-Sight Probability for Channel Modeling in Typical Indoor Environments. *IEEE Antennas Wirel. Propag. Lett.* **2018**, *17*, 1359–1362. [CrossRef]
28. Basnayaka, C.M.W.; Jayakody, D.N.K.; Chang, Z. Age-of-Information-Based URLLC-Enabled UAV Wireless Communications System. *IEEE Internet Things J.* **2022**, *9*, 10212–10223. [CrossRef]
29. Ma, Z.; He, C.; Rao, Y.; Jiang, J.; Ma, S.; Gao, F.; Xing, L. Time- and Power-Splitting Strategies for Ambient Backscatter System. *IEEE Access* **2019**, *7*, 40068–40077. [CrossRef]
30. Zhang, R.; Xiong, K.; Lu, Y.; Gao, B.; Fan, P.; Letaief, K.B. Joint Coordinated Beamforming and Power Splitting Ratio Optimization in MU-MISO SWIPT-Enabled HetNets: A Multi-Agent DDQN-Based Approach. *IEEE J. Sel. Areas Commun.* **2022**, *40*, 677–693. [CrossRef]
31. Li, Z.; Chen, W.; Wu, Q.; Wang, K.; Li, J. Joint Beamforming Design and Power Splitting Optimization in IRS-Assisted SWIPT NOMA Networks. *IEEE Trans. Wirel. Commun.* **2022**, *21*, 2019–2033. [CrossRef]
32. Park, G.; Lee, K. Optimization of the Trajectory, Transmit Power, and Power Splitting Ratio for Maximizing the Available Energy of a UAV-Aided SWIPT System. *Sensors* **2022**, *22*, 9081. [CrossRef]
33. Jiang, W.; Rahman, B.M.A. Design of Power-Splitter with Selectable Splitting-Ratio Using Angled and Cascaded MMI-Coupler. *IEEE J. Quantum Electron.* **2018**, *54*, 6300509. [CrossRef]
34. Ruan, T.; Chew, Z.J.; Zhu, M. Energy-Aware Approaches for Energy Harvesting Powered Wireless Sensor Nodes. *IEEE Sens. J.* **2017**, *17*, 2165–2173. [CrossRef]
35. Huang, F.; Chen, J.; Wang, H.; Ding, G.; Gong, Y.; Yang, Y. Multiple-UAV-Assisted SWIPT in Internet of Things: User Association and Power Allocation. *IEEE Access* **2019**, *7*, 124244–124255. [CrossRef]
36. Khan, N.A.; Awang, A.; Karim, S.A.A. Security in Internet of Things: A Review. *IEEE Access* **2022**, *10*, 104649–104670. [CrossRef]

Disclaimer/Publisher's Note: The statements, opinions and data contained in all publications are solely those of the individual author(s) and contributor(s) and not of MDPI and/or the editor(s). MDPI and/or the editor(s) disclaim responsibility for any injury to people or property resulting from any ideas, methods, instructions or products referred to in the content.